A LOCKING-FREE QUADRATIC NURBS-BASED ISOGEOMETRIC FORMULATION FOR PLATES ANALYSIS

by Thai Hoang Chien[1] - Nguyen Xuan Hung[2] - Nguyen Thoi Trung[2]

ABSTRACT

A new Reissner-Mindlin plate formulation based on a quadratic NURBS-based isogeometric is presented. In order to avoid the transverse shear locking and to improve the accuracy of the present formulation, the quadratic NURBS-based isogeometric is incorporated with the Mixed Interpolation of Tensorial Components (MITC) technique to give a so-called quadratic NURBS-based isogeometric Mixed Interpolation of Tensorial Components method (Nurbs-MITC9). Numerical results of the proposed formulation show excellent performance compared to other available approaches.

Keywords: Isogeometric analysis, Non-Uniform Rational B-splines (NURBS), MITC, Reissner-Mindlin plate.

1. INTRODUCTION

The Reissner–Mindlin (R-M) plate model is written in terms of the out-of-plane displacement and the rotation to the mid-plane. The R-M model is widely utilized for the thin and thick plates/shells. It allows the use of simple approximations of transverse displacement and rotation to the mid plane. Commonly, the R-M plate model usually is subjected to so-called shear locking phenomenon when the plate becomes very thin (the thickness of plate tends to zero). The mixed formulation is in general often used to overcome this drawback. In this formulation, a new independent variable is additionally introduced into the shear strain. It is suitably approximated correspond to some properties of reduction operator [1, 2].

In development of advanced computational methodologies, Hughes *et al*. [3] have recently proposed a NURBS-based isogeometric analysis to bridge the gap between Computer Aided Design (CAD) and Finite Element Analysis (FEA). Isogeometric analysis is thus very promising because it can directly use Non-Uniform Rational B-splines (NURBS) to describe both exact geometry and approximate solution. For structural mechanics, isogeometric analysis has been extensively studied for nearly incompressible linear and non-linear elasticity and plasticity problem [4], structural vibrations [5], the Reissner-Mindlin plate/shell [6, 7], Kirchhoff-Love shell [8, 9, 10] and the large deformation with rotation-free [11], etc.

In this paper, we propose a new mixed quadratic Nurbs-based isogeometric method for the R-M plate. The idea is that the shear strains are approximated by independent interpolation functions in natural coordinates while the bending strains still remain as the classical formulation. The present method is locking-free and improves the accuracy of solutions compared to the classical

[1]*Division of Computational Mechanics, Ton Duc Thang University HCM.*

[2]*Department of Mechanics, Faculty of Mathematics and Computer Science, University of Science HCM.*

quadratic Nurbs-based isogeometric. In this study, we focus on the Nurbs-MITC9 element for the static analysis of isotropic R-M plates.

The paper is arranged as follows: a brief of the B-spline and NURBS surface is described in section 2. Section 3 presents an isogeometric approximation for Reissner-Mindlin plates. Several numerical examples are illustrated in section 4. Finally we close our paper with some concluding remarks.

2. NURBS - BASED ISOGEOMETRIC ANALYSIS FUNDAMENTALS

2.1. Knot Vectors and Basis Functions

In one-dimensional problems, a knot vector Ξ is the set of coordinates in the parametric space as

$$\boldsymbol{\Xi} = \left\{\xi_1, \xi_2, ..., \xi_{n+p+1}\right\} \tag{1}$$

where p, n are the order of the B-Spline and the number of basis functions associated with control points, respectively. The interval $[\xi_1 \ \xi_{n+p+1}]$ is called a patch. Given a knot vector, the B-spline basis functions $N_{i,p}(\xi)$ of order $p = 0$ are defined recursively on the corresponding knot vector as follows

$$N_{i,0}(\xi) = \begin{cases} 1 & if \quad \xi_i < \xi < \xi_{i+1} \\ 0 & \text{otherwise} \end{cases} \tag{2}$$

The basis functions of p>1 are defined by the following recursion formula:

$$N_{i,p}(\xi) = \frac{\xi - \xi_i}{\xi_{i+p} - \xi_i} N_{i,p-1}(\xi) + \frac{\xi_{i+p+1} - \xi}{\xi_{i+p+1} - \xi_{i+1}} N_{i+1,p-1}(\xi) \text{ with } p>1 \tag{3}$$

2.2. NURBS Surface

The B-spline curve is defined as

$$\mathbf{C}(\xi) = \sum_{i=1}^{n} N_{i,p}(\xi)\mathbf{P}_i \tag{4}$$

where $\mathbf{P}_i$ are the control points and $N_{i,p}$ (ξ) is the pth-degree B-spline basis function defined on the open knot vector.

The B-spline surfaces are defined by the tensor product of basis functions in two parametric dimensions ξ and η with two knot vectors Ξ $=\{\xi_1, \xi_2 ..., \xi_{n+p+1}\}$ and H $=\{\eta_1, \eta_2 ..., \eta_{m+q+1}\}$ are expressed as follows:

$$\mathbf{S}(\xi,\eta) = \sum_{i=1}^{n}\sum_{j=1}^{m} N_{i,p}(\xi) M_{j,q}(\eta)\mathbf{P}_{i,j} \tag{5}$$

where $\mathbf{P}_{i,j}$ is the bidirectional control net, $N_{i,p}(\xi)$ and $M_{j,q}(\eta)$ are the B-spline basis functions defined on the knot vectors over an $n \times m$ net of control points $\mathbf{P}_{i,j}$. Eq. (5) is rewritten in the same form as the finite element method

$$\mathbf{S}(\xi,\eta) = \sum_{A}^{nm} N_A(\xi,\eta)\mathbf{P}_A \tag{6}$$

where $N_A(\xi,\eta) = N_{i,p}(\xi)M_{j,q}(\eta)$ is the shape function associated with node A.

Similar to B-Splines, a NURBS surface is defined as

$$\mathbf{S}(\xi,\eta) = \sum_{A=1}^{nm} R_A(\xi,\eta)\mathbf{P}_A \tag{7}$$

where $R_A = N_A w_A / \sum_A^{nm} N_A w_A$ and w_A are the rational basis functions and the weight functions, respectively.

Let w, $\boldsymbol{\beta} = \{\beta_x \ \beta_y\}^T$ be the transverse displacement of the mid-plane, the rotations in the y-z and x-z planes, respectively. The displacements of any point in the Reissner-Mindlin (R-M) plates can be expressed as [12]:

3. THE QUADRATIC NURBS-BASED ISOGEOMETRIC FORMULATION FOR PLATES

$$u(x,y,z) = z\beta_x \ ; \ v(x,y,z) = z\beta_y \ \ and \ \ w(x,y,z) = w \tag{8}$$

The bending strains through the following equation:

$$\boldsymbol{\varepsilon} = [\varepsilon_{xx} \ \ \varepsilon_{yy} \ \ \gamma_{xy}]^T = z\boldsymbol{\kappa} = z\left[\beta_{x,x} \quad \beta_{y,y} \quad \beta_{x,y} + \beta_{y,x}\right]^T \tag{9}$$

and transverse shear strains are basically defined as

$$\boldsymbol{\gamma}^{DI} = \left[\gamma_{xz} \ \ \gamma_{yz}\right]^T = \nabla w + \boldsymbol{\beta} = \left[w_{,x} + \beta_x \quad w_{,y} + \beta_y\right]^T \tag{10}$$

A weak form of the static for R-M plates can be briefly expressed as:

$$\int_\Omega \delta\boldsymbol{\kappa}^T \mathbf{D}^b \boldsymbol{\kappa} \mathrm{d}\Omega + \int_\Omega \left(\delta\boldsymbol{\gamma}^{DI}\right)^T \mathbf{D}^s \boldsymbol{\gamma}^{DI} \mathrm{d}\Omega = \int_\Omega \delta w p d\Omega \tag{11}$$

where

$$\mathbf{D}^b = \frac{Et^3}{12(1-\nu^2)}\begin{bmatrix} 1 & \nu & 0 \\ \nu & 1 & 0 \\ 0 & 0 & \dfrac{1-\nu}{2} \end{bmatrix} \quad , \quad \mathbf{D}^s = \frac{kE}{2(1+\nu)}\begin{bmatrix} 1 & 1 \\ 1 & 1 \end{bmatrix} \tag{12}$$

Using the same NURBS basis functions, the displacement is interpolated as:

$$\mathbf{u}^h(\xi,\eta) = \sum_A^{nm} \mathbf{R}_A(\xi,\eta)\mathbf{q}_A \tag{13}$$

where $n \times m$ is the number basis functions. $\mathbf{R}_A(\xi,\eta)$ and $\mathbf{q}_A = [w_A \ \beta_{xA} \ \beta_{yA}]^T$ are rational basic functions and the degrees of freedom of $\mathbf{u}^h$ associated to control point A, respectively.

The strains in Eq. (9) and (10) can be expressed to following nodal displacements as:

$$\left[\boldsymbol{\varepsilon} \ \ \boldsymbol{\gamma}^{DI}\right]^T = \sum_{A=1}^{nm}\left[\mathbf{B}_A^b \quad \mathbf{B}_A^{s-DI}\right]^T \mathbf{d}_A = \sum_{A=1}^{nm} \mathbf{B}_A \mathbf{d}_A \tag{14}$$

where

$$\mathbf{B}_A^b = \begin{bmatrix} 0 & R_{A,x} & 0 \\ 0 & 0 & R_{A,y} \\ 0 & R_{A,y} & R_{A,x} \end{bmatrix} \quad \text{and} \quad \mathbf{B}_A^{s-DI} = \begin{bmatrix} R_{A,x} & R_A & 0 \\ R_{A,y} & 0 & R_A \end{bmatrix} \tag{15}$$

Where, the strain-displacement matrix $\mathbf{B}_A^{s-DI}$ is calculated with the direct from displacement field.

The formulation of a R-M plates can then be obtained for static analysis

$$\mathbf{Kq} = \mathbf{f} \tag{16}$$

where the global stiffness matrix is

$$\mathbf{K} = \int_\Omega \left(\mathbf{B}_A^b\right)^T \mathbf{D}^b \mathbf{B}_A^b \mathrm{d}\Omega + \int_\Omega \left(\mathbf{B}_A^{s-DI}\right)^T \mathbf{D}^s \mathbf{B}_A^{s-DI} \mathrm{d}\Omega \tag{17}$$

and the force matrix also is written as

$$\mathbf{f} = \int_\Omega R_A p \mathrm{d}\Omega \tag{18}$$

where **K,** **f** and **q** are the global stiffness matrix, the force matrix and the displacement matrix, respectively.

In FEM, locking appears in low-order elements. Shear locking will disappear for the interpolation functions of order 5 or higher [13]. Similar to FEM, the quadratic NURBS-based elements are still locking when the plate becomes very thin. This is due to shear affects remaining in the stiffness formulation. To overcome this drawback, we propose a new formulation that relies on independent interpolation fields in the natural coordinate system for the approximation of the shear strains as given in Bathe and Dvorkin [14].

$$\boldsymbol{\gamma}^{ANS}(x,y) = \mathbf{J}^{-1}\boldsymbol{\gamma}^{ANS}\left(\bar{\xi},\bar{\eta}\right) \quad \text{where} \quad \boldsymbol{\gamma}^{ANS}\left(\bar{\xi},\bar{\eta}\right) = \sum_{k=1}^{ntp} \boldsymbol{\gamma}^{DI}\left(\bar{\xi}_k,\bar{\eta}_k\right)\mathbf{h}\left(\bar{\xi},\bar{\eta}\right) \tag{19}$$

where γ^{ANS}, γ^{DI}, **J** and $\mathbf{h}\left(\bar{\xi},\bar{\eta}\right)$ are the assumed natural strain (ANS) matrix, the strain matrix direct calculated from the displacement, the Jacobian matrix and the interpolation shape functions in the natural coordinate at the tying points, respectively. To compute the Jacobian determinant of mapping from the parent element to the physical space as shown Figure 1, **J** is calculated as

$$\mathbf{J} = \frac{1}{4}\begin{vmatrix} \dfrac{\partial x}{\partial \xi} & \dfrac{\partial y}{\partial \xi} \\ \dfrac{\partial x}{\partial \eta} & \dfrac{\partial x}{\partial \eta} \end{vmatrix} \tag{20}$$

Figure 1. The physical element is first bulled back to the parametric domain, and then mapping to the parent element.

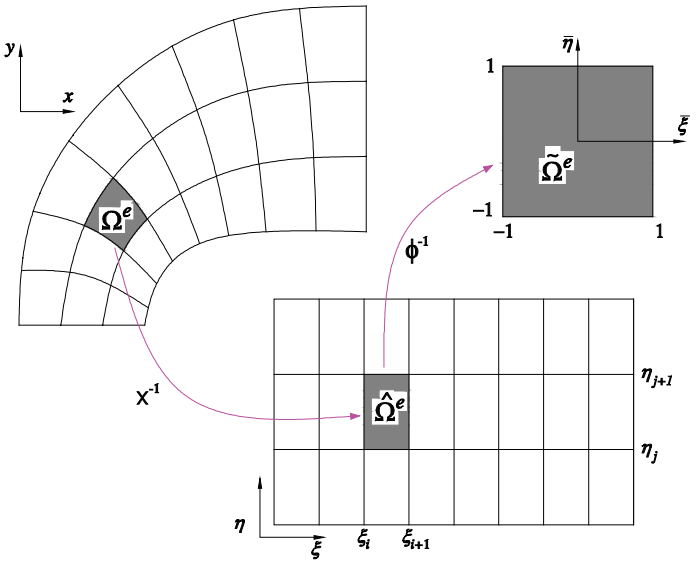

The Nurbs-MITC9 element uses nine tying points *k* depending on strains. Shape functions for the nine-node elements are needed for approximating the strains at those tying points shown as Figure 2. Then, we obtain the displacement – shear strain matrix as follows:

$$\mathbf{B}_A^{s-ANS} = \mathbf{J}^{-1}\begin{bmatrix} \sum_{k=1}^{ntp} R_{A,\xi}\left(\bar{\xi}_k,\bar{\eta}_k\right)h_k\left(\bar{\xi},\bar{\eta}\right) & \sum_{k=1}^{ntp} N_A\left(\bar{\xi}_k,\bar{\eta}_k\right)h_k\left(\bar{\xi},\bar{\eta}\right) & 0 \\ \sum_{k=1}^{ntp} N_{A,\eta}\left(\bar{\xi}_k,\bar{\eta}_k\right)h_k\left(\bar{\xi},\bar{\eta}\right) & 0 & \sum_{k=1}^{ntp} N_A\left(\bar{\xi}_k,\bar{\eta}_k\right)h_k\left(\bar{\xi},\bar{\eta}\right) \end{bmatrix} \tag{21}$$

The global stiffness matrix from (17) is therefore changed as follows:

$$\mathbf{K} = \int_\Omega \left(\mathbf{B}_A^b\right)^T \mathbf{D}^b \mathbf{B}_A^b \mathrm{d}\Omega + \int_\Omega \left(\mathbf{B}_A^{s-ANS}\right)^T \mathbf{D}^s \mathbf{B}_A^{s-ANS} \mathrm{d}\Omega \tag{22}$$

Figure 2. Strain interpolations $\gamma_{\bar{\xi}t}$, $\gamma_{\bar{\eta}t}$ and tying points of the Nurbs-MITC9.

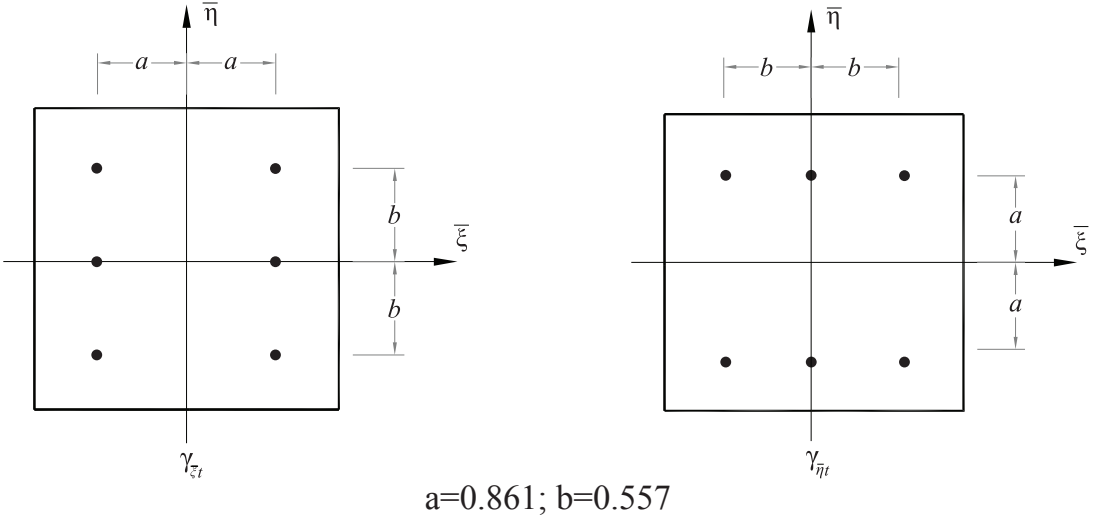

a=0.861; b=0.557

4. NUMERICAL RESULTS

In this section, we illustrate two examples for analysis of the isotropic R-M plates using Nurbs-MITC9 element. The full integration (3x3 integration points) is used for this element. A shear correction factor of k=5/6 is fixed for all computations. To analyze the effectiveness of the method, the square and circular plates with fully supported and clamped boundary conditions are considered.

4.1. Fully clamped square plate

First, we consider a square plate (length L, thickness h) with fully clamped boundary conditions, subjected to a uniform load p = 1 as shown in Figure 3. The material parameters are: Young's modulus E =10^7, Poisson's ratio v = 0.3 and the length to thickness ratios L/h = 10^2, 10^3, 10^4, 10^5 and 10^6. Due to symmetry, only the below left quadrant of the plate is modeled with 4, 8, 16 and 32 the quadratic NURBS element. The exact displacement and the bending moment at center of plate are given by Taylor and Auricchio [15] as:

$$\bar{w} = \frac{10^3 D}{qL^4} w(0,0) \quad \text{and} \quad \bar{M}_x = \frac{10^2}{qL^2} M_x(0,0)$$

Figure 4 shows the normalized deflection and bending moment of the clamped plates with the length to thickness ratios L/h = 100. The results of the present method are compared with exact solution [15]. It can be seen that the solutions of the Nurbs-MITC9 converge faster than the quadratic Nurbs to the exact solutions. Now we illustrate the performance of the present element when the plate becomes very thin. Theoretically, it is well known that the shear effect reduces as the ratio of length-thickness (L/h) increases. Hence, solutions of Reissner-Mindlin theory will approach those of Kirchhoff model. Figure 5 depicts the central deflection and moment of plates with respect to the change of ratios L/h using the Nurbs-MITC9 and the quadratic Nurbs. It is observed that the quadratic Nurbs elements are subjected to shear locking in the thin plate limit, e.g., $L/h \geq 100$. As shown, shear locking problem is solved very well corresponding to the Nurbs-MITC9 element. It can be seen from Figure 5 that the Nurbs-MITC9 elements perform very well when the plate becomes very thin.

Figure 3. Geometry of square fully-clamped plates.

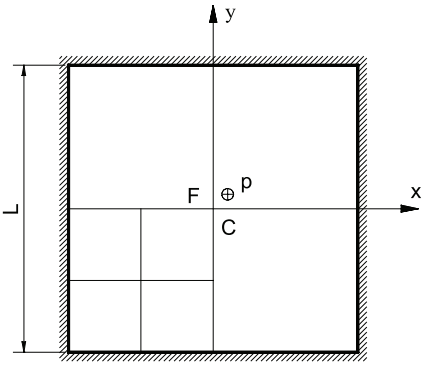

Figure 4. Center displacement and bending moment of square clamped plates with *L*/t=100.

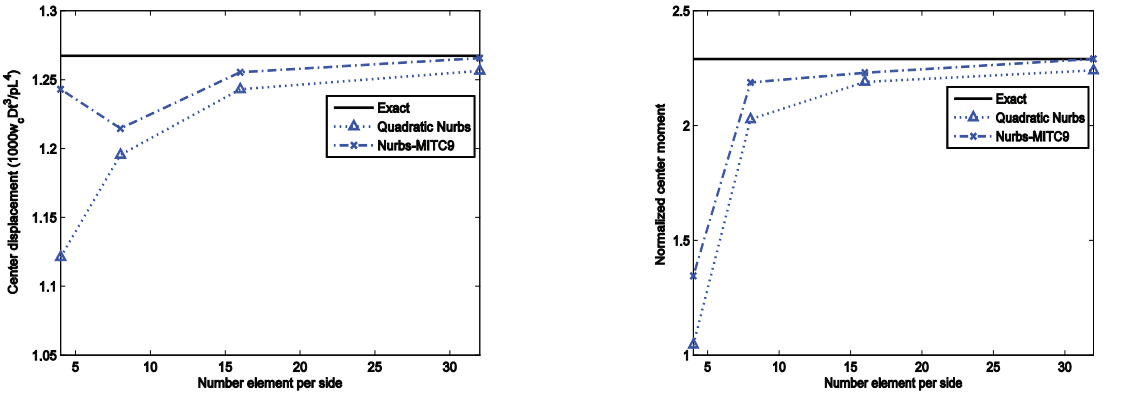

Figure 5. Center displacement and moment of square clamped plates with various *L*/t ratio.

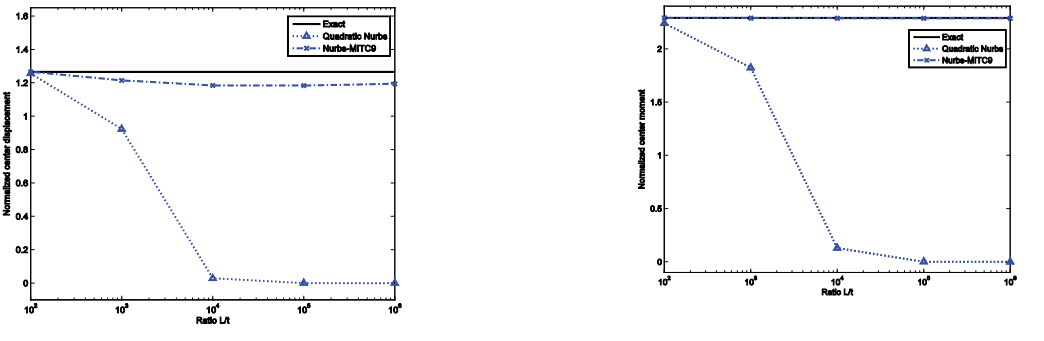

4.2. Circular plates

Let us now consider an isotropic circular plate under uniform transverse loading. We analyze both the fully-clamped and simply-supported cases, respectively.

4.2.1. Fully-clamped Case

Let us consider a fully-clamped circular plate of radius R = 0.5, as illustrated in Figure 6. A rational quadratic basis is used to describe a circle. The coarsest mesh, Ξ×H, is defined by the knot vectors as follows **Ξ** ={0 0 0 1 1 1}; **H** ={0 0 0 1 1 1}. The exact geometry is represented with a single element using 9 control points, as shown in Figure 7. The four meshes used in the analysis are plotted in Figure 8. The exact displacement and bending moment at the center of the circular plate are given [16] as:

$$w(0,0)=\left(\frac{qR^4}{64D}\right) \quad \text{and} \quad M_x(0,0)=(1+\nu)\left(\frac{qR^2}{16}\right)$$

Normalization solutions are taken with respect to the exact displacement and the exact bending moment.

Normalized center displacement and bending moment of circular fully clamped plates with *L*/*t*=100 are plotted in Figure 9. The Nurbs-MITC9 element is more accurate than the quadratic Nurbs element and is in very good agreement with the exact solution. When the length/thickness ratio $L/t \rightarrow \infty$, the displacement and bending moment of the present method still converge

to the exact solution while the quadratic Nurbs element exhibits shear locking. The convergence of the displacement and bending moment of the circular plates with various lengths to thickness ratios are illustrated as show Figure 10.

Figure 6. Geometry of circular plates.

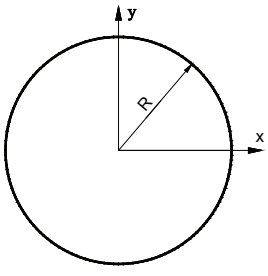

Figure 7. Mesh and control net for a disk of radius R=0.5: (a) coarse mesh and (b) control net.

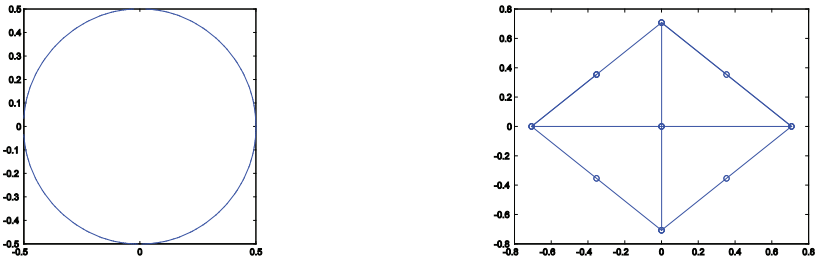

Figure 8. Meshes produced by h-refinement (knot insertion).

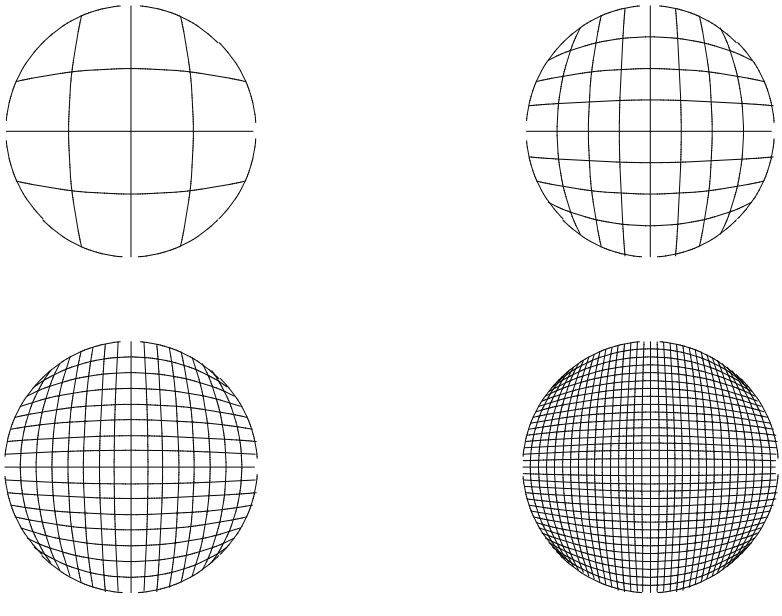

Figure 9. Normalized center displacement and bending moment of circular fully clamped plates with L/t=100.

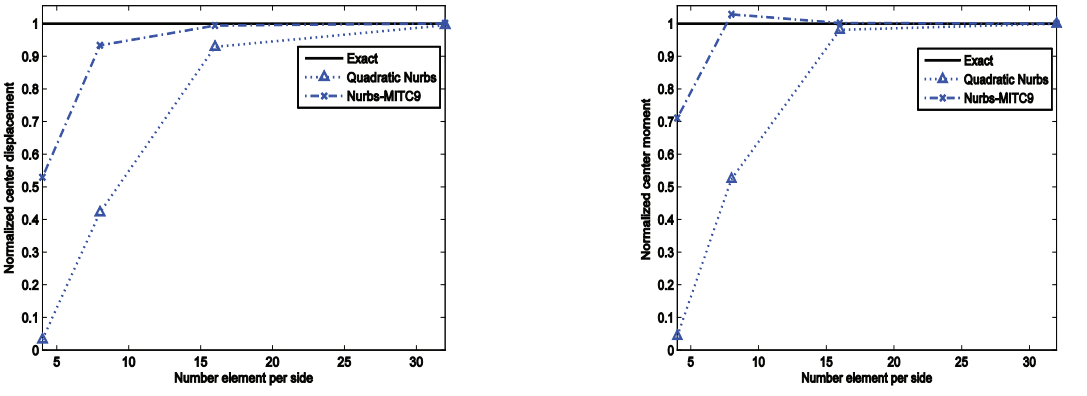

4.2.2. Simply-Supported Case

Finally, let's consider a simply-supported circle plate of radius R=0.5. The exact Kirchhoff solutions for this problem are given by [16]:

$$w(0,0)=\left(\frac{5+\nu}{1+\nu}\right)\left(\frac{qR^4}{64D}\right) \quad \text{and} \quad M_x(0,0)=(3+\nu)\left(\frac{qR^2}{16}\right)$$

The center displacement and moment of plate are also the normalization. Now we illustrate the case of the length/thickness ratio $L/t \to \infty$. Figure 11 shows the convergence of the displacement and moment at the center of plate. It is again seen that the present method is locking-free when the plate becomes very thin. The quadratic Nurbs element is locking when the thickness of plate tends to zeros.

5. CONCLUSION

A new Reissner-Mindlin plate formulation based on a quadratic NURBS-based isogeometric has proposed for static analysis of plates. The present element is locking-free when the plate becomes very thin. The performance of the present element is improved compared to the original quadratic Nurbs element. The results of the proposed method are in excellent agreement with the exact solution.

Figure 10. Normalized center displacement and moment of circular fully clamped plates with various L/t ratios.

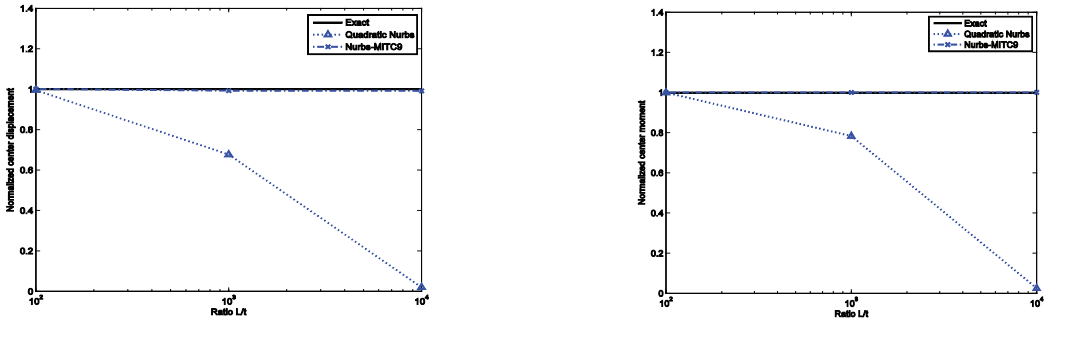

Figure 11. Normalized center displacement and moment of circular fully supported plates with various *L*/t ratios.

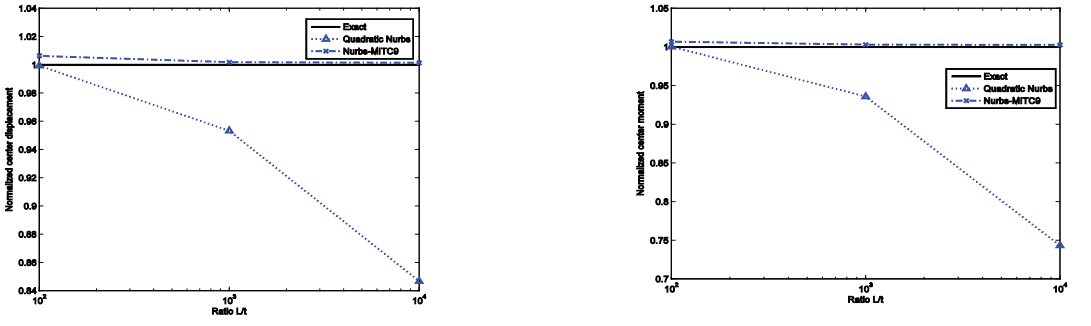

REFERENCES

1. F. Brezzi, M. Fortin and R. Stenberg. Error analysis of mixed-interpolated elements for Reissner Mindlin plates, Mathematical Models and Methods in Applied Sciences 1 (1991) 125–151.
2. R. Duran and E. Liberman. On mixed finite element methods for the Reissner–Mindlin plate model. Mathematics of Computation 58 (1992) 561–573.
3. T.J.R. Hughes, J.A. Cottrell, and Y. Bazilevs. Isogeometric analysis: CAD, finite elements, NURBS, exact geometry and mesh refinement. Computer Methods in Applied Mechanics and Engineering 194 (2005) 4135–4195.
4. T. Elguedj, Y. Bazilevs, V. Calo, T. Hughes. B and F projection methods for nearly incompressible linear and non-linear elasticity and plasticity using higher-order nurbs elements. Computer Methods in Applied Mechanics and Engineering 197 (2008) 2732–2762.
5. J.A. Cottrell, A. Reali, Y. Bazilevs, and T.J.R. Hughes. Isogeometric analysis of structural vibrations. Computer Methods in Applied Mechanics and Engineering 195 (2006) 5257–5296.
6. L.B. Veiga, A. Buffa, C. Lovadina, M. Martinelli and G. Sangalli. An isogeometric method for the Reissner-Mindlin plate bending problem. Computer Methods in Applied Mechanics and Engineering, in press, doi:10.1016/j.cma.2011.10.009.
7. D.J. Benson, Y. Bazilevs, M.C. Hsu, T.J.R. Hughes. Isogeometric shell analysis: The Reissner–Mindlin shell. Computer Methods in Applied Mechanics and Engineering 199 (2010) 276–289.
8. J. Kiendl, K.U. Bletzinger, J. Linhard, R. Wuchner. Isogeometric shell analysis with Kirchhoff-Love elements. Computer Methods in Applied Mechanics and Engineering 198 (2009) 3902–3914.
9. J. Kiendl, Y. Bazilevs, M.C. Hsu, R. Wchner, and K.U. Bletzinger. The bending strip method for isogeometric analysis of Kirchhoff-Love shell structures comprised of multiple patches. Computer Methods in Applied Mechanics and Engineering 199 (2010) 2403–2416.

10. N. Nguyen-Thanh, J. Kiendl, H. Nguyen-Xuan, R. Wüchner, K.U. Bletzinger, Y. Bazilevs and T. Rabczuk. Rotation free isogeometric thin shell analysis using PHT-splines. *Computer Methods in Applied Mechanics and Engineering* 200 (2011) 3410--3424.
11. D.J. Benson, Y. Bazilevs, M.C. Hsu, and T.J.R. Hughes. A large deformation, rotation-free, isogeometric shell. Computer Methods in Applied Mechanics and Engineering 200 (2011) 1367–1378.
12. E. Reissner. The effect of transverse shear deformations on the bending of elastic plates. Journal of Applied Mechanics 12 (1945) A69–A77.
13. R. Kouhia. On stabilized finite element methods for the Reissner-Mindlin plate model. International Journal for Numerical Methods in Engineering 74 (2008) 1314–1328.
14. K.J. Bathe and E.N. Dvorkin. A four-node plate bending element based on Mindlin/Reissener plate theory and a mixed interpolation. International Journal for Numerical Methods in Engineering 21 (1985) 367–383.
15. R.L. Taylor and F. Auricchio. Linked interpolation for Reissner-Mindlin plate elements. Part I- A simple triangle. International Journal for Numerical Methods in Engineering 36 (1993) 3056–3066.
16. J. N. Reddy. Theory and Analysis of Elastic Plates and Shells. CRC Press, Taylor & Francis Group, Boca Raton, 2007.